"Virtual"-Power-Hardware-in-the-Loop Simulations for Crosswind Kite Power with Ground Generation

Florian Bauer[1], *Member, IEEE*, Christoph M. Hackl[2], *Member, IEEE*, Keyue Smedley[3], *Fellow, IEEE*
and Ralph M. Kennel[4], *Senior Member, IEEE*

Abstract— **Major parts of a crosswind kite power system based on the ground generation principle can be tested without risks to the kite in a laboratory or workshop by coupling the winch(es) to loads, which emulate the kite's forces (power-hardware-in-the-loop, PHIL). As such tests can be costly and time consuming, this paper proposes an intermediate step: Instead of emulating the computed kite loads on a coupled real load, they are emulated on the existent electrical drives of the winches. With less effort, the winches turn similarly as if they where loaded by a real kite. As the loads are virtually present only, but hardware is involved, one may call this principle "virtual"-PHIL. Measurements with a small-scale prototype are presented.**

I. Motivation

Kites, or tethered wings, are promising alternatives to ground based wind turbines for harvesting wind energy (see e.g. [1]–[3] and references therein): As shown in Fig. 1, a kite made of soft materials like a paraglider or alternatively made of rigid materials like a sail plane is tethered to one or more winches on the ground, where each is connected to an electrical drive. The kite is flown in crosswind motions with a high lift force and pulls the tether(s) from the winch(es). Energy is generated by operating the electrical drive(s) as generator(s) through regenerative braking. When the maximum tether length is reached, the kite is flown to a low force position like the zenith, and/or pitched down, and reeled back in. A rigid kite can also dive towards the

[1]Florian Bauer is Ph.D. candidate at the Institute for Electrical Drive Systems and Power Electronics, Technische Universität München, Arcisstrasse 21, 80333 Munich, Germany, florian.bauer@tum.de, corresponding author.

[2]Christoph M. Hackl is Senior Researcher and the Head of Research Group "Control of renewable energy systems" at the Munich School of Engineering, Technische Universität München, c/o Wind Energy Institute, Boltzmannstrasse 15, 85748 Garching, Germany.

[3]Keyue Smedley is Professor at The Henry Samueli School of Engineering, Power Electronics Laboratory, University of California, Irvine, CA, 92697.

[4]Ralph M. Kennel is Professor at the Institute for Electrical Drive Systems and Power Electronics, Technische Universität München, Arcisstrasse 21, 80333 Munich, Germany.
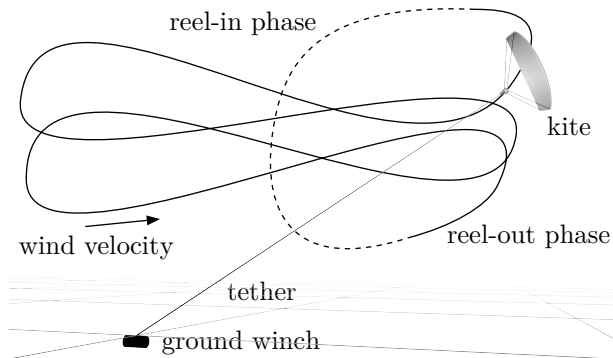
Fig. 1. Illustration of crosswind kite power with ground generation.

ground winch(es) for minimal reel-in time. During the reel-in phase, only a fraction of the generated energy is dissipated by operating the electrical drive(s) as motor(s). If more than one winch and drive is used, the winches are also (partly) responsible to steer the kite on the flight path.

Compared to conventional wind power, crosswind kite power promises to harvest wind energy in higher altitudes with stronger and steadier wind by needing only a fraction of the construction material. Hence, it promises to have a higher capacity factor, lower capital investments, and in the end a lower Levelized Cost Of Electricity. A mechanical output power of $2\,\mathrm{MW}$ was already achieved by a commercial soft kite by SkySails [4].

Hardware-in-the-Loop (HIL) simulations or power-HIL (PHIL) simulations, respectively, are essential for a cost-effective development, particularly for this technology as a failure can cause a crash and loss of the kite. One PHIL simulation possibility is shown in Fig. 2 [5]: The tether(s)

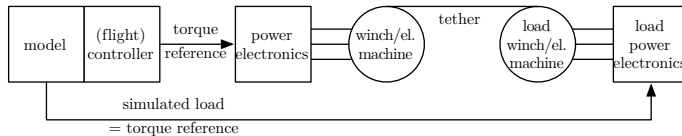Fig. 2. Power-Hardware-in-the-Loop for crosswind kite power with ground generation.

of the winch(es) of the ground station are connected to load winch(es) with load electrical drive(s) to emulate the loads of the kite, which are computed by a simulation model. Consequently, control algorithms can be tested with the complete ground station hardware under full power without risks to the kite. Moreover, failure modes can be found with

reduced effort at any weather condition in a laboratory or workshop. However, this PHIL simulation setup imposes difficulties: (i) The load winch contributes a rather high inertia that might be not present if a kite was attached. (ii) A rather complex load must be designed and constructed, which has a higher rated torque and power than the winch(es) under test to account for losses, and which has its own tether guidance system. (iii) Provisions for tether breaks must be made to minimize risks to the testing personal. (iv) High replacement costs and delays can emerge when failures lead to uncontrolled tether entanglement around the equipment. (v) To avoid (ii)–(iv), a load drive could be coupled directly to the shaft of a winch to emulate the kite loads. However, this could increase design costs or is (almost) impossible e.g. if the electrical machines and winches are one integrated assembly without shaft extension.

As a cost- and time-saving alternative or preliminary step of the described PHIL, this paper proposes to use the existent electrical drive(s) to also emulate the load torque(s). As a consequence, the winch(es) behave/turn as if tether(s) of a kite were pulling, but despite loss and inertial torques, torques are only existent in software and thus "virtual". As (power-) hardware is tested, but only small power flows emerge, let us call this method "virtual"-PHIL (VPHIL).

Applying virtual loads to an electrical drive has been proposed previously in [6], [7] for a BLDC motor. This study generalizes and extends the concepts to a general electrical drive with constraints and applies it for crosswind kite power with ground generation as well as shows its benefits for this application. The contribution of this study can be summarized as follows: (i) Proposal and classification of VPHIL simulations for crosswind kite power with ground generation as example. (ii) Mathematical problem description of the drive control for crosswind kite power with ground generation. (iii) Description of a proposed VPHIL solution. (vi) Exemplary demonstration of VPHIL on a small-scale three-winch prototype with simulation/measurement results.

This paper is organized as follows: Sec. II classifies VPHIL in view of other "in-the-loop" simulations. Sec. III formulates the problem and Sec. IV proposes a solution. Measurement results from a small-scale prototype are shown in Sec. V. Finally, conclusions are given in Sec. VI.

II. CLASSIFICATION

Fig. 3 visualizes possible "in-the-loop"-simulations applied for an electrical drive (see also e.g. [8] and references therein): Model-in-the-Loop (MIL) is a dynamic simulation of the developed controller and a simulation model. In Software-in-the-Loop (SIL) the controller is implemented and tested in the target programming language and controls a software model which is either written in the same programming language or interfaced via a communication interface. In Hardware-in-the-Loop (HIL) a part of the hardware is involved, but usually only on signal level: E.g. a signal generator emulates measured electrical signals for the power electronics in the same format as voltage sensors, current sensors or encoders would output. The next step would be the

Fig. 3. "In-the-Loop" simulations for electrical drives. Paths and blocks which involve higher power are drawn thicker.

proposed VPHIL simulation followed by PHIL. The final test case can also be called Plant-in-the-Loop (PIL). MIL, SIL and HIL allow the testing of the controller without risks to equipment and testing personal. Particularly, possible crashes of the kite happen only in a software model. In VPHIL the risks are still small, since almost only the rotational energies of the winches are involved.

III. PROBLEM DESCRIPTION

In the following, a simplified crosswind kite power model comprising an electrical drive model is derived. Fig. 4 (uncolored parts) shows the block diagram representation of the derived equations.

Fig. 4. Block diagram of a crosswind kite power model comprising an electrical drive model (uncolored parts) and proposed VPHIL solution (green modification), where the kite dynamics and loads are simulated.

A. Shaft Dynamics of a Winch/Electrical Drive

The shaft dynamics can be described by Newton's axioms

$$\dot{L}(t) = M_\Sigma(t), \qquad L(t_0) = L_0 \qquad (1)$$
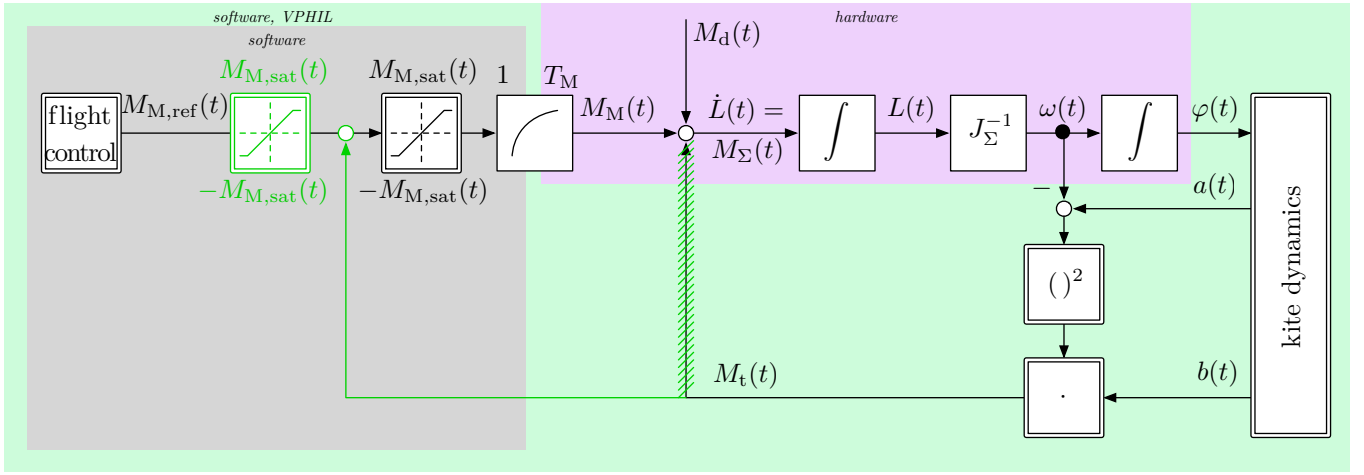
$$\dot{\varphi}(t) = \underbrace{J_\Sigma^{-1} L(t)}_{=:\omega(t)}, \qquad \varphi(t_0) = \varphi_0 \qquad (2)$$

with torque sum $M_\Sigma(t) \in \mathbb{R}\,[\mathrm{Nm}]$ at time $t \in \mathbb{R}\,[\mathrm{s}]$, angular momentum $L(t) \in \mathbb{R}\,[\mathrm{kg\,m^2/s}]$, initial angular momentum $L_0 \in \mathbb{R}\,[\mathrm{kg\,m^2/s}]$ at initial time $t_0 \in \mathbb{R}\,[\mathrm{s}]$, inertia sum $J_\Sigma \in \mathbb{R}\,[\mathrm{kg\,m^2}]$, angular velocity $\omega(t) \in \mathbb{R}\,[\mathrm{rad/s}]$, angular position $\varphi(t) \in \mathbb{R}\,[\mathrm{rad}]$ and initial angular position $\varphi_0 \in \mathbb{R}\,[\mathrm{rad}]$. As the winch and the electrical machine (possibly with a gearbox) are attached to the shaft, the torque sum is

$$M_\Sigma(t) = M_\mathrm{M}(t) + M_\mathrm{t}(t) + M_\mathrm{d}(t) \qquad (3)$$

with machine torque $M_\mathrm{M}(t) \in \mathbb{R}\,[\mathrm{Nm}]$, tether torque from the winch $M_\mathrm{t}(t) \in \mathbb{R}\,[\mathrm{Nm}]$ and disturbance torque $M_\mathrm{d}(t) \in \mathbb{R}\,[\mathrm{Nm}]$ which comprises e.g. friction. If a gearbox is used, $M_\mathrm{M}(t)$ would be scaled by the gear ratio, but is not considered here.

The torques $M_\mathrm{M}(t)$ and $M_\mathrm{t}(t)$ are further derived in the next subsections.

B. Tether Torque/Kite

The tether torque is given by

$$M_\mathrm{t}(t) = r(t) F_\mathrm{t}(t) \qquad (4)$$

with tether force $F_\mathrm{t}(t) \in \mathbb{R}\,[\mathrm{N}]$ and winch radius $r(t) \in \mathbb{R}\,[\mathrm{m}]$, which can be time dependent if the tether is wound up in several layers. A simplified expression for the tether force can be found with the following assumption:

Assumption 1: *Gravitational and inertial forces are small compared to aerodynamic forces, i.e. $m_\mathrm{k} + m_\mathrm{t} \approx 0$ with kite mass $m_\mathrm{k} \in \mathbb{R}\,[\mathrm{kg}]$ and tether mass $m_\mathrm{t} \in \mathbb{R}\,[\mathrm{kg}]$. Furthermore, the tether is straight. Consequently, the aerodynamic force generated by the kite $F_\mathrm{ae}(t) \in \mathbb{R}\,[\mathrm{N}]$*

and the tether force $F_\mathrm{t}(t)$ are in balance, i.e. $F_\mathrm{t}(t) = F_\mathrm{ae}(t)$.

The tether force is then given by

$$F_\mathrm{t}(t) = \frac{1}{2}\rho(t)A\Big(\cos\big(\psi(t)\big)\cos\big(\theta(t)\big)v_\mathrm{w}(t) - v_\mathrm{t}(t)\Big)^2$$
$$\frac{\sqrt{C_\mathrm{L}(t)^2 + C_{\mathrm{D},\Sigma}(t)^2}^3}{C_{\mathrm{D},\Sigma}(t)^2} \qquad (5)$$

with air density $\rho(t) \in \mathbb{R}\,[\mathrm{kg/m^3}]$, the kite's characteristic (projected wing-) area $A \in \mathbb{R}\,[\mathrm{m^2}]$, azimuth angle $\psi(t) \in \mathbb{R}\,[\mathrm{rad}]$ (i.e. angle between tether projected to ground and wind), elevation angle $\theta(t) \in \mathbb{R}\,[\mathrm{rad}]$ (i.e. angle between tether and ground), wind speed $v_\mathrm{w}(t) \in \mathbb{R}\,[\mathrm{m/s}]$, tether speed $v_\mathrm{t}(t) \in \mathbb{R}\,[\mathrm{m/s}]$, lift coefficient $C_\mathrm{L}(t) \in \mathbb{R}\,[1]$ and drag coefficient sum $C_{\mathrm{D},\Sigma}(t) \in \mathbb{R}\,[1]$ (compare e.g. with [2, Chap. 2, Eq. 2.30]). Inserting

$$\omega(t) = \frac{v_\mathrm{t}(t)}{r(t)} \qquad (6)$$

$$a(t) := \frac{\cos\big(\psi(t)\big)\cos\big(\theta(t)\big)v_\mathrm{w}(t)}{r(t)} \qquad (7)$$

$$b(t) := \frac{1}{2}\rho(t)Ar(t)^3 \frac{\sqrt{C_\mathrm{L}(t)^2 + C_{\mathrm{D},\Sigma}(t)^2}^3}{C_{\mathrm{D},\Sigma}(t)^2} \qquad (8)$$

into (5) and then into (4) yields

$$M_\mathrm{t}(t) = b(t)\big(a(t) - \omega(t)\big)^2, \qquad (9)$$

where $a(t)$ and $b(t)$ are time dependent functions.

Note, if multiple winches are used on ground, $F_\mathrm{t}(t)$ is distributed among the winches and only leads to a (slightly) modified function $b(t)$.

C. Electrical Drive with Torque Control: SMPMSM as Example

In the following a surface mounted permanent magnet synchronous machine (SMPMSM) is modeled as one example of an electrical machine type. Similar results can be found for

other types of electrical machines. The results are generalized in the next subsection. The following information can be found similarly in a standard text book on electrical drives (see e.g. [9], [10]).

The following assumption(s) are imposed on the SMPMSM:

Assumption 2: *Magnetomotive force and magnetic flux are distributed radially only (i.e. the machine is regarded 2D) and radially sinusoidal (fundamental wave model). Moreover, the magnetic properties are linear, current independent and direction independent (d-inductance is equal to q-inductance and constant), no eddy currents are regarded, all parameters are independent of the temperature and all windings have identical properties.*

The stator current dynamics of a SMPMSM in the field oriented reference frame "k" with abscissa d and ordinate q is then given by

$$\frac{\mathrm{d}}{\mathrm{d}t}i_{\mathrm{s}}^{\mathrm{d}}(t) = \frac{1}{L_{\mathrm{s}}}\big(u_{\mathrm{s}}^{\mathrm{d}}(t) - R_{\mathrm{s}}i_{\mathrm{s}}^{\mathrm{d}}(t) \underbrace{+ p\omega(t)L_{\mathrm{s}}i_{\mathrm{s}}^{\mathrm{q}}(t)}_{*}\big) \qquad (10)$$

$$\frac{\mathrm{d}}{\mathrm{d}t}i_{\mathrm{s}}^{\mathrm{q}}(t) = \frac{1}{L_{\mathrm{s}}}\big(u_{\mathrm{s}}^{\mathrm{q}}(t) - R_{\mathrm{s}}i_{\mathrm{s}}^{\mathrm{q}}(t) \underbrace{- p\omega(t)L_{\mathrm{s}}i_{\mathrm{s}}^{\mathrm{d}}(t) - p\omega(t)\Psi_{\mathrm{PM}}}_{*}\big) \qquad (11)$$

with initial conditions

$$i_{\mathrm{s}}^{\mathrm{d}}(t_0) = i_{\mathrm{s},0}^{\mathrm{d}} \quad \text{and} \quad i_{\mathrm{s}}^{\mathrm{q}}(t_0) = i_{\mathrm{s},0}^{\mathrm{q}}, \qquad (12)$$

where $i_{\mathrm{s}}^{\mathrm{d}}(t), i_{\mathrm{s},0}^{\mathrm{d}}, i_{\mathrm{s}}^{\mathrm{q}}(t), i_{\mathrm{s},0}^{\mathrm{q}} \in \mathbb{R}\,[\mathrm{A}]$ are the (initial) d- and q-currents, $L_{\mathrm{s}} \in \mathbb{R}\,[\mathrm{H}]$ is the inductance, $u_{\mathrm{s}}^{\mathrm{d}}(t), u_{\mathrm{s}}^{\mathrm{q}}(t) \in \mathbb{R}\,[\mathrm{V}]$ are the d- and q-voltages, $R_{\mathrm{s}} \in \mathbb{R}\,[\Omega]$ is the resistance, $p \in \mathbb{R}\,[1]$ is the number of pole pairs, and $\Psi_{\mathrm{PM}} \in \mathbb{R}\,[\mathrm{Vs}]$ is the permanent magnet flux linkage. The machine torque (air gap torque) is given by

$$M_{\mathrm{M}}(t) = \frac{3}{2}p\Psi_{\mathrm{PM}}i_{\mathrm{s}}^{\mathrm{q}}(t). \qquad (13)$$

PI field oriented control for the d- and the q-currents, with disturbance rejection (of the terms marked with * in (10)–(11)), is considered. For a simplified model of the drive, the following additional assumption is made:

Assumption 3: *No voltage saturation is regarded, i.e. the output of the current controllers $u_{\mathrm{s}}^{\mathrm{d}}(t), u_{\mathrm{s}}^{\mathrm{q}}(t)$ are not saturated. Moreover, the voltages are applied without delay.*

Assumption 3 implies a linear dynamic behavior and is valid for small $\omega(t)$ compared to the rated speed. Moreover, field weakening is not regarded, so that the d-current reference is always zero, $i_{\mathrm{s,ref}}^{\mathrm{d}}(t) = 0$. In view of (13), the reference for the q-current is then set to

$$i_{\mathrm{s,ref}}^{\mathrm{q}}(t) = \frac{M_{\mathrm{M,ref}}(t)}{\frac{3}{2}p\Psi_{\mathrm{PM}}}, \qquad (14)$$

where $M_{\mathrm{M,ref}}(t) \in \mathbb{R}\,[\mathrm{Nm}]$ is the reference torque from a superimposed controller. It can be shown that $i_{\mathrm{s,ref}}^{\mathrm{q}}(t)$ and thus $M_{\mathrm{M,ref}}(t)$ are tracked with a first-order delay.

To keep the currents within safe bounds (e.g. within the rated current), $i_{\mathrm{s,ref}}^{\mathrm{q}}(t)$, or equivalently $M_{\mathrm{M,ref}}(t)$, is saturated, i.e. (14) is replaced by

$$i_{\mathrm{s,ref}}^{\mathrm{q}}(t) = i_{\mathrm{s,ref,sat}}^{\mathrm{q}}(t) = \frac{M_{\mathrm{M,ref,sat}}(t)}{\frac{3}{2}p\Psi_{\mathrm{PM}}} \qquad (15)$$

with

$$M_{\mathrm{M,ref,sat}}(t) = \begin{cases} M_{\mathrm{M,sat}}(t) & \text{for } M_{\mathrm{M,ref}}(t) > M_{\mathrm{M,sat}}(t) \\ -M_{\mathrm{M,sat}}(t) & \text{for } M_{\mathrm{M,ref}}(t) < -M_{\mathrm{M,sat}}(t) \\ M_{\mathrm{M,ref}}(t) & \text{else} \end{cases} \qquad (16)$$

where $M_{\mathrm{M,ref,sat}}(t) \in \mathbb{R}\,[\mathrm{Nm}]$ is the saturated torque reference and $M_{\mathrm{M,sat}}(t) \in \mathbb{R}\,[\mathrm{Nm}]$ is the saturation (maximal achievable) torque (which can be time dependent).

D. Generalized Electrical Drive Model

Similar relations and controllers can be found for most other types of electrical machines which motivates the formulation of a generalized electrical drive model: The reference torque is saturated and tracked with a first order delay, i.e. (10)–(15) can be replaced by

$$\dot{M}_{\mathrm{M}}(t) = \frac{1}{T_{\mathrm{M}}}\big(M_{\mathrm{M,ref,sat}}(t) - M_{\mathrm{M}}(t)\big), \quad M_{\mathrm{M}}(t_0) = M_{\mathrm{M},0}, \qquad (17)$$

where $T_{\mathrm{M}} \in \mathbb{R}_{>0}\,[\mathrm{s}]$ is a time constant and $M_{\mathrm{M},0} \in \mathbb{R}\,[\mathrm{Nm}]$ is the initial torque. Note that this model has validity in a wide operation range, also if parts of Assumptions 2–3 are not made.

E. Problem of Virtual-Power-Hardware-in-the-Loop

The VPHIL problem can be formulated as follows: Find a system setup where $M_{\mathrm{t}}(t)$ is computed by a software model and only virtually applied to the (real) electrical drive with minimal hardware efforts but similar resulting system behavior.

IV. PROPOSED SOLUTION

A. Virtual Load Torque Addition

The block diagram of Fig. 4 visualizes the proposed solution as green modification: $M_{\mathrm{t}}(t)$ is computed by a software model of the kite and added virtually (in software) to $M_{\mathrm{M,ref}}(t)$, instead at the winch (as real mechanical torque). The torque reference from the flight controller is (additionally) saturated to the maximum machine torque, since this would be the limit for the real machine in the real application. This method can be seen as if the existing drive also generates the load.

B. Torque Reference Saturation Within the Flight Controller

Within the "flight control" block in Fig. 4, $M_{\mathrm{M,ref}}(t)$ may be further saturated: As an example, a tether can only sustain tension but no compression. Consequently, it is meaningful that the flight controller outputs only negative torques (if negative angular velocity corresponds to reeling-in), i.e.

$$M_{\mathrm{M,ref}}(t) \in \mathbb{R}_{<0}. \qquad (18)$$

Such measures have no effect on the proposed VPHIL solution.

C. Virtual Machine Torque, Virtual Current and Virtual Power for a SMPMSM

As the electrical machine is turning as if it was loaded by a kite, machine torque, q-current and power have a real component and a virtual component (in the following marked by ~). Instead of the real values, the total virtual values (i.e. real component plus virtual component, in the following marked by ^) must be used as feedback, e.g. for the flight controller to control the (total virtual) power of the winch(es).

The true machine torque component of a SMPMSM is given by (13) whereas the virtual component is equal to

$$\tilde{M}_{\mathrm{M}}(t) = -M_{\mathrm{t}}(t), \tag{19}$$

where $M_{\mathrm{t}}(t)$ is computed by the simulation model of the kite. The total virtual machine torque is

$$\hat{M}_{\mathrm{M}}(t) = M_{\mathrm{M}}(t) + \tilde{M}_{\mathrm{M}}(t) = \frac{3}{2}p\Psi_{\mathrm{PM}}i_{\mathrm{s}}^{\mathrm{q}}(t) - M_{\mathrm{t}}(t). \tag{20}$$

Similarly, the real component of the q-current is present in the power electronics and machine and is measured by the current sensors, whereas the virtual component can be expressed by

$$\tilde{i}_{\mathrm{s}}^{\mathrm{q}}(t) = \frac{-M_{\mathrm{t}}(t)}{\frac{3}{2}p\Psi_{\mathrm{PM}}} \tag{21}$$

leading to a total virtual q-current of

$$\hat{i}_{\mathrm{s}}^{\mathrm{q}}(t) = i_{\mathrm{s}}^{\mathrm{q}}(t) + \tilde{i}_{\mathrm{s}}^{\mathrm{q}}(t) = i_{\mathrm{s}}^{\mathrm{q}}(t) + \frac{-M_{\mathrm{t}}(t)}{\frac{3}{2}p\Psi_{\mathrm{PM}}}. \tag{22}$$

Finally, the real component of the (mechanical) power is

$$P(t) = M_{\mathrm{M}}(t)\omega(t) \tag{23}$$

whereas the virtual component is

$$\tilde{P}(t) = -M_{\mathrm{t}}(t)\omega(t) \tag{24}$$

and the total virtual power is

$$\hat{P}(t) = P(t) + \tilde{P}(t) = \big(M_{\mathrm{M}}(t) - M_{\mathrm{t}}(t)\big)\omega(t). \tag{25}$$

D. Discussion

The proposed solution is valid for small T_{M} and fast measurements of $\omega(t)$ and $\varphi(t)$, which is usually the case as T_{M} and the measurement times are in the magnitude of milliseconds. Further, the proposed solution is valid if

$$-M_{\mathrm{M,sat}}(t) \leq M_{\mathrm{M,ref}}(t) + M_{\mathrm{t}}(t) \leq M_{\mathrm{M,sat}}(t), \tag{26}$$

which is also usually the case, as the real torque is only used to overcome inertia and losses in the drive. Consequently, the system behaves similarly to a real loaded system with a kite (assuming a good kite model). Only small energies like the rotational energy of the winches are involved, but testing the winches and controllers up to full speed is possible, also with advanced concepts such as field weakening.

Note that unlike HIL and PHIL, the proposed VPHIL does not require any additional hardware such as a signal generator or a load generator (and the necessary interfacing), see Fig. 3.

It should also be noted that in-between HIL and VPHIL in Fig. 3 an unloaded test could be added, which would be the same as the proposed VPHIL solution with $M_{\mathrm{t}}(t) = 0$. However, such a test has only limited value: If a saturation in the flight controller as in (18) is applied, the test will not work as the tether(s) can only be reeled-in. Moreover, as the measured power is small, no power control can be tested. Consequently, the system's behavior can be much different from the real system with kite, contrary to the proposed VPHIL simulation.

V. IMPLEMENTATION AND MEASUREMENTS WITH A SMALL-SCALE PROTOTYPE

VPHIL is being applied to test a small-scale crosswind kite power ground station prototype in the author's laboratory, before testing the system with a kite in the field.

A. Hardware and Software Setup

Fig. 5 shows a photograph of the small-scale ground station prototype developed by the authors at the University of California, Irvine. The ground station consists of three

Fig. 5. VPHIL laboratory setup of the small-scale three-winches ground station prototype.

winches with direct drive hub SMPMSMs mounted to an aluminum frame and each connected to an inverter. The inverters are connected to a host computer via a USB-serial interface. The host computer executes the flight controller and the simulation model with $100\,\mathrm{Hz}$ control cycle frequency. The microcontroller on each inverter executes the field oriented PI current controllers as well as velocity controllers with $8\,\mathrm{kHz}$ control cycle frequency and $16\,\mathrm{kHz}$ switching frequency. The currents in the three phases, the DC link voltage and the electrical position from binary hall sensors (i.e. the measured position is discretized in $\frac{2\pi}{6}$ rad-steps) are measured. The position, the angular velocity and the load torque are estimated by a Kalman Filter on each inverter's microcontroller.

B. Results

Fig. 6 shows example VPHIL simulation results of a complete "pumping cycle" (reel-out and reel-in phases) for a $6\,\mathrm{m}^2$-test kite at $4\,\mathrm{m/s}$ wind speed. The upper graph shows the 3D flight path.

The first time series shows the tether torques. As no tethers are connected, the real tether torques (light) are zero, while the virtual ones (dark) were computed by the simulation model.

As visible in the second time series, the real machine torques (light) are (slightly) above zero during reeling-out and (slightly) below zero during reeling-in. The real machine torques overcome (real) friction, whereas the virtual ones (dark) counteract the virtual tether torques. The noise of the real machine torques result from the measurement noise of the q-currents from which they are computed with (13).

The third time series shows the measured mechanical angular velocities and the forth time series shows the measured mechanical angular positions. In those plots, it is visible how the winches are responsible for both, generating power and steering the kite by applying differential tether lengths.

VI. CONCLUSIONS

This paper proposes VPHIL as preliminary step or alternative to PHIL. Within the research and development carried out by the authors with a small-scale prototype, VPHIL proved to be cost-effective and time saving, particularly by detecting faults and implementation errors of the drive control and of the communication links. VPHIL is relatively easy to apply, as it involves only slight software modifications and no signal generator (as in HIL) or load generator (as in PHIL) with corresponding necessary interfacing. The advantages of VPHIL are likely higher for a full scale kite power system, as the efforts and safety measures for PHIL simulations would be increased. Note that VPHIL is an option for many electrical drive control applications. However, compared to PHIL, it is particularly beneficial for this application as it allows relatively simple testings of the system in a laboratory or workshop without complex load winches. Nevertheless, the system is not tested under full power, so that failures caused by higher power flows cannot be detected by VPHIL.

REFERENCES

[1] M. Loyd, "Crosswind kite power," *Journal of Energy*, vol. 4, no. 3, pp. 106–111, 1980.

[2] U. Ahrens, M. Diehl, and R. Schmehl, Eds., *Airborne Wind Energy*, ser. Green Energy and Technology. Springer Berlin Heidelberg, 2013. [Online]. Available: http://link.springer.com/book/10.1007%2F978-3-642-39965-7

[3] L. Fagiano and M. Milanese, "Airborne wind energy: An overview," in *American Control Conference (ACC)*. IEEE, June 2012, pp. 3132–3143.

[4] M. Erhard and H. Strauch, "Control of towing kites for seagoing vessels," *IEEE Transactions on Control Systems Technology*, vol. 21, no. 5, pp. 1629–1640, Sept 2013.
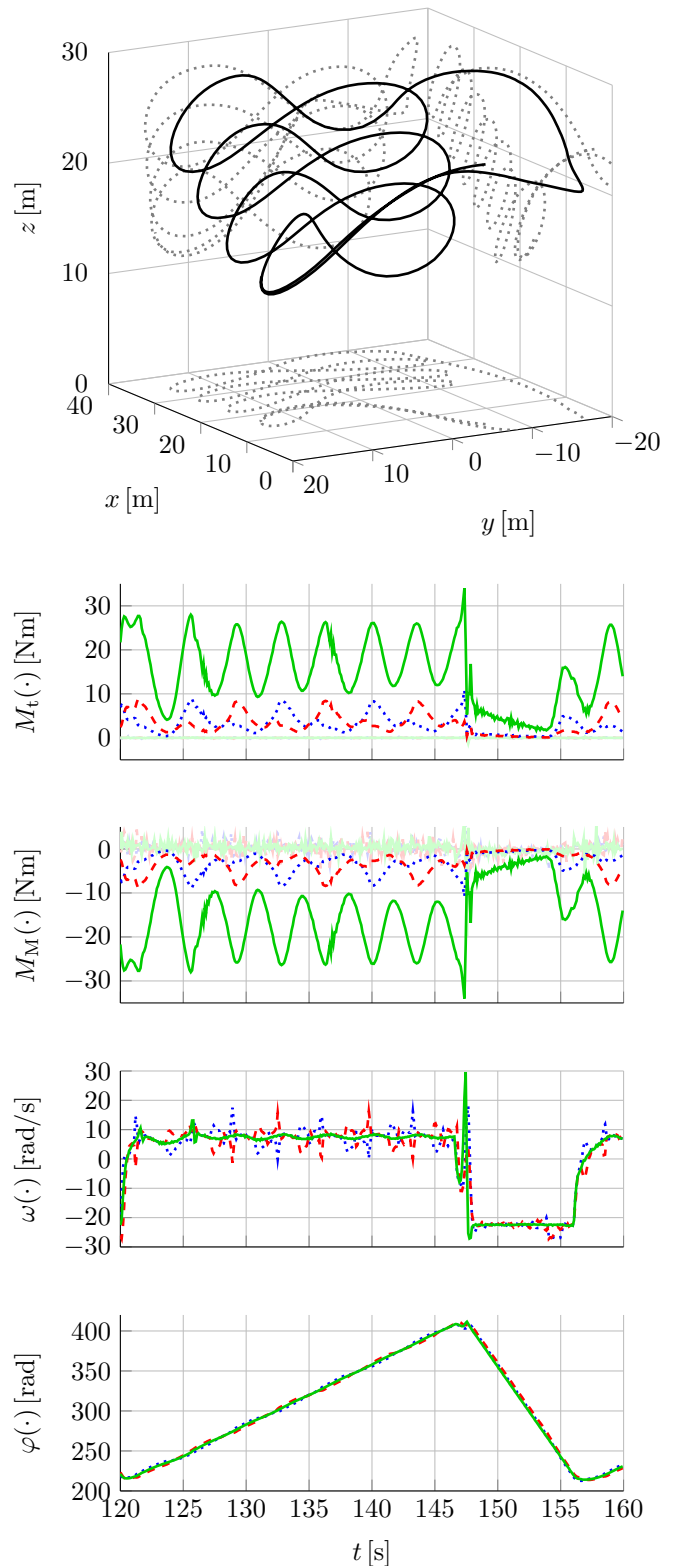
Fig. 6. Example VPHIL simulation results: On top is the kite's position trajectory with positions $x, y, z \in \mathbb{R}\,[\mathrm{m}]$. Below are time series of the winch values: real load torques $M_\mathrm{t}(t)$ in light and virtual ones $\tilde{M}_\mathrm{t}(t)$ in dark, real machine torques $M_\mathrm{M}(t)$ in light and virtual ones $\tilde{M}_\mathrm{M}(t)$ in dark, measured mechanical angular velocities $\omega(t)$, measured mechanical angular positions $\varphi(t)$. Graphs for the left winch are - - -, for the right winch are ⋯⋯ and for the middle winch are ——.

[5] Damian Aregger et al., "Hardware in the loop testing for autonomous airborne wind energy systems," in *The International Airborne Wind Energy Conference 2015: Book of abstracts*. TU Delft/Roland Schmehl, 2015.

[6] A. Kuperman and R. Rabinovici, "Virtual torque and inertia loading of controlled electric drive," *Education, IEEE Transactions on*, vol. 48, no. 1, pp. 47–52, Feb 2005.

[7] A. Kuperman, "Hil-based virtual disturbance and parameter variations of controlled electric drive," in *Industrial Electronics, 2008. ISIE 2008. IEEE International Symposium on*, June 2008, pp. 2165–2170.

[8] A. Bouscayrol, "Different types of hardware-in-the-loop simulation for electric drives," in *Industrial Electronics, 2008. ISIE 2008. IEEE International Symposium on*, June 2008, pp. 2146–2151.

[9] K. H. Nam, *AC Motor Control and Electrical Vehicle Applications*. CRC Press, 2010.

[10] C. Dirscherl, C. Hackl, and K. Schechner, "Modellierung und Regelung von modernen Windkraftanlagen: Eine Einführung *(available at the authors upon request)*," in *Elektrische Antriebe – Regelung von Antriebssystemen*, D. Schröder, Ed. Springer-Verlag, 2015, ch. 24, pp. 1540–1613.